Attractors of low$-Rm$ MHD turbulence

By Alban Pothérat[1] and Thierry Alboussière[2]

[1]Ilmenau Technical University, Kirchoffstr. 1 98693 Ilmenau, Germany

[2]Laboratoire de Géophysique Interne et Tectonophysique, CNRS, Observatoire de Grenoble, Université Joseph Fourier
Maison des Géosciences, BP 53, 38041 Grenoble Cedex 9, France

(Received 14 March 2006)

Low R_m MHD turbulence is investigated here through estimates of upper bounds for attractor dimension. A flow between two parallel walls with an imposed perpendicular magnetic field is considered. The flow is defined by its maximum velocity and the intensity of the magnetic field. Given the corresponding Reynolds and Hartmann numbers, one can derive rigourously an upper bound for the dimension of the turbulent attractor and find out which modes must be chosen to achieve this bound. This is then used heuristically to estimate the size of the smallest turbulent vortices and the degree of anisotropy of the turbulence. Our upper bound derivation is based on known bounds of the non-linear inertial term, while low R_m Lorentz forces – being linear – can be easily dealt with.

The simple configuration considered in this paper allows us to model three important previously identified transitions. The first is the transition from classical to MHD turbulence when anisotropy takes the form of a "Joule cone". Second, one can define the transition from 3D MHD turbulence to quasi-2D MHD turbulence, when all "Sommerfeld modes" disappear and only "Squire modes" are left. Third, Hartmann layers undergo transition to turbulence when more than one "boundary layer mode" exists in the attractor.

In addition to this 3D approach, we also determine upper bounds for the dimension of turbulent flows modelled using a 2D MHD equation, which should become physically relevant in the quasi-2D MHD regime. The advantage of this 2D approach is that, while upper bounds are quite loose in three dimensions, optimal upper bounds exist for the nonlinear term. This allows us to derive realistic attractor dimensions for quasi-2D MHD flows.

1. Introduction

Magnetohydrodynamic turbulence at low magnetic Reynolds number is relevant to many laboratory-scale experiments (**?**) as well as to many industrial processes (**?**). This is a consequence of the small values of liquid metal Prandtl numbers Pm, around 10^{-6}. With human-scale magnetic fields in the range 0.1 to 1 Tesla, and human-scale size and flow velocity, it is likely that Lorentz forces will have a great impact on liquid metal flow turbulence and unlikely that the flow will affect the imposed magnetic field, as magnetic diffusivity exceeds kinematic viscosity by a factor $Pm^{-1} = 10^6$. Unexpectedly, magnetohydrodynamic turbulence can also be relevant to large magnetic Reynolds numbers when the magnetic Prandtl number is small. This is the case for the geodynamo, for which the magnetic Prandtl number is about 10^{-6}. In this case, going from large eddies to smaller ones, the magnetic turbulent cascade stops long before the hydrodynamic cascade. The small scales of large-Rm turbulence can thus be considered as an example of low-Rm

turbulence.

The question of how turbulence looks like can be addressed theoretically in a number of ways, most of them based on physical assumptions or turbulence model. It is possible to make no assumption and although this leads to limited information, this is reliable information on which further studies can be based, for instance the derivation of a turbulence model. In this paper, we have estimated upper bounds for the attractor dimension of low-Rm MHD turbulent flows. This work is based on previous non-MHD studies of Navier-Stokes attractors in three and two dimensions. It has been shown that the attractor of turbulent solutions is of finite dimension even though the set of possible functions is of infinite dimension. This is basically due to viscous effects setting a maximum curvature to possible solutions. In three dimensions, the fundamental questions of the smoothness of solutions of Navier-Stokes equations and of the existence of a compact attractor remain open. We assume this is the case and this constitutes the only assumption. We do not need to make such assumptions for the two-dimensional case as smoothness has been proven. In addition, previous upper bounds of attractor dimensions for two dimensional flows coincide very nearly with heuristic estimates based on the cascade of enstrophy ; . This is not the case for three dimensional rigourous upper bounds as they are found to be much larger than heuristic estimates based on the cascade of energy ; .

Our main goal is basically to extend the non-MHD studies to the case of low-Rm MHD. As Lorentz forces are linear forces, this does not include additional theoretical difficulties. However, as these forces are strongly dissipative, the final upper bounds for attractor dimensions are significantly affected when imposing a magnetic field. Togother with the upper bounds, we put in evidence the modes that would constitute the attractor when those bounds are achieved. We then determine whether one can model well-known transitions between different turbulent states when increasing the imposed magnetic field. The chosen configuration study is taken as simple as possible to enable us to shown these transitions: the electrically conducting fluid is contained between two parallel infinite walls, and a perpendicular magnetic field is applied. First, it is expected that isotropic turbulence becomes anisotropic by stretching in the direction of the magnetic field, secondly a quasi two dimension regime is obtained, thirdly the turbulent Hartmann boundary layers developing on the walls become laminar.

All three transitions can be observed and determine formally by analyzing rigourous upper bounds for attractor dimension and the corresponding set of vector-valued functions. The first transition is defined by the absence of functions with variations along the magnetic field direction outside (Hartmann) boundary layers with no variation in the perpendicular directions. The second transition occurs when this absence is independent of any condition regarding perpendicular variations. Finally the third transition corresponds to the presence of other flow length-scales close to the walls than the laminar Hartmann layer thickness.

The method of estimates of dimension upper bounds for attractors is presented in section 2. Section 3 is devoted to the determination of least dissipative modes. In section 4 and 5 we determine the attractor dimension of three dimensional and two dimensional turbulent flows respectively and discuss the various transitions observed as the nature of turbulence changes with the intensity of the magnetic field. Comments on this work and results are presented in the final section 6.

2. Method to determine dimension and modes of the attractor

From the point of view of dynamical systems, the phase space of turbulence is the infinite-dimensional set of all vector-valued functions in which Navier-Stokes solutions evolve as time goes on. If the attractor is compact, its finite dimension d can be determined in the following way. Any solution to the Navier-Stokes equations should eventually become arbitrarily close to the attractor. Let us then consider an infinitesimal n-dimensional box around a solution. As time passes, each point in the box evolves according to the Navier-Stokes equations. Then, eventually, this box will end up within the attractor. This provides a criterion on the fate of the volume of the box: if $n > d$ the volume of the box will converge towards zero, in the same way as a cube has to have a vanishing volume if it has to fit in a surface of zero thickness. As soon as $n < d$ the volume of the box will not converge towards zero, *i. e.* it will not converge, converge towards a finite value, or diverge – should ergocicity hold – as the box spreads into the whole attractor .

The evolution of the size of n-dimensional infinitesimal boxes is intimately related to the Lyapunov exponents. The n-th Lyapunov exponent is the maximal rate of growth of the n-th dimensional volume spanned by n infinitesimal disturbances about a solution at large time (*i.e.* in the attractor). Denoting $\mathcal{A}$ the linearized Navier-Stokes equations, a disturbance $\delta\mathbf{u}$ about a solution $\mathbf{u}$ obeys the following equation :

$$\frac{\partial}{\partial t}\delta\mathbf{u} = \mathcal{A}(\mathbf{u})\delta\mathbf{u} + \mathcal{O}(\delta\mathbf{u}^2). \tag{2.1}$$

Considering n disturbances spanning a n-volume $V_n = \|\delta\mathbf{u}_1 \times \cdots \times \delta\mathbf{u}_n\|$, the equation for a single disturbance (2.1) can be generalized and integrated to provide an expression for V_n (see):

$$V_n(t) = V_n(0) \exp\left(t \left\langle Tr\left[\mathcal{A}P_n\right]\right\rangle\right), \tag{2.2}$$

where P_n denotes the projection onto the n-dimensional subspace spanned by the n disturbances at initial time, and the bracket $<>$ stands for long time-average. If the n disturbances are perpendicular eigenvalues, the trace of the evolution operator is simply the sum of the individual eigenvalues. We shall use this property to determine the trace as the linearized Navier-Stokes operator being self-adjoint possesses a basis of perpendicular eigenfunctions. For each integer value n, we determine the n largest eigenvalues and consider whether their sum is larger or smaller than zero. In the first case, n is smaller than the attractor dimension, in the second case, n is larger than the attractor dimension.

Non-linear terms can stretch solutions and are pushing eigenvalues towards positive values, while dissipative terms make solutions shrink (in phase space) and lead to negative eigenvalues. The largest eigenvalues are obtained for large scale functions while small scales vector fields produce more dissipation and thus negative eigenvalues. Hence, large scale motions are selected first to calculate the first Lyapunov exponents. Their number is limited though and eventually one has to select negative eigenvalues. Eventually, when enough negative values are added up, they balance the initial positive eigenvalues and Lyapunov exponents themselves become negative. The n-th Lyapunov exponent for which this happens is roughly the dimension of the turbulent attractor†.

The above cross products and projection require the existence of a scalar product in the phase space of vector valued functions (in 2D or 3D space). In this study we shall use the standard L^2 Hilbert structure. Given $\mathbf{u}$ and $\mathbf{v}$ two vector fields, their scalar product

† These dimensions are larger numbers compared to one, so we do not need to worry very long about their exact non-integer value between $n-1$ and n. For low-dimensional attractors, the Kaplan-Yorke formula can be used to determine this value precisely **?**.

is defined as:

$$\mathbf{u}.\mathbf{v} = \int_{\mathcal{V}} u_i v_i^* dV, \tag{2.3}$$

where $i = 1, 2$ or $i = 1, 2, 3$ for 2D or 3D turbulence.

If one considers a small perturbation, the following equations govern its evolution:

$$\partial_t \delta\mathbf{u} = -\nabla\delta p - \mathbf{u}.\nabla\delta\mathbf{u} - \delta\mathbf{u}.\nabla\mathbf{u} + \nu(\nabla^2 + \frac{\sigma B^2}{\rho\nu}\nabla^{-2}\partial_{zz}^2)\delta\mathbf{u} \tag{2.4}$$

$$\nabla \cdot \delta\mathbf{u} = 0 \tag{2.5}$$

with associated boundary conditions for the perturbation:

$$\forall \mathbf{x} \in \mathbf{R}^3, \forall k_x, k_y \in Z,$$

$$\mathbf{v}(\mathbf{x}) = \mathbf{v}(\mathbf{x} + k_x L\mathbf{e}_x) = \mathbf{v}(\mathbf{x} + k_y L\mathbf{e}_y) \tag{2.6}$$

$$\mathbf{v}(z = -L) = \mathbf{v}(z = L) = 0 \tag{2.7}$$

The perturbation in electric current $\delta\mathbf{j}$ is related to $\delta\mathbf{u}$ by

$$\delta\mathbf{j} = -\sigma B\nabla^{-2}\partial_z \nabla \times \delta\mathbf{u} \tag{2.8}$$

and must satisfy the perturbed form of the electric current conservation $\nabla\cdot\delta\mathbf{j} = 0$ as well as the condition that the walls located at $z = -L$ and $z = L$ are electrically insulating:

$$\delta j_n = 0 \tag{2.9}$$

where e and σ_W are the thickness and electrical conductivity of the thin wall.

The trace of the evolution operator is split into non-linear and linear parts, $\mathcal{A}(\mathbf{u})\delta\mathbf{u} = \mathcal{B}(\mathbf{u}, \delta\mathbf{u}) + \mathcal{L}(\delta\mathbf{u})$. For any disturbance $\delta\mathbf{u}$ of norm unity, the contribution of the non linear term to the trace operator is expressed as:

$$\int_{\mathcal{V}} \delta\mathbf{u}.\mathcal{B}(\mathbf{u}, \delta\mathbf{u})dV = \int_{\mathcal{V}} \delta\mathbf{u}.\left[-\nabla\delta p - \mathbf{u}.\nabla\delta\mathbf{u} - \delta\mathbf{u}.\nabla\mathbf{u}\right] dV \tag{2.10}$$

It has been shown in that this contribution can be bounded as follows:

$$\begin{aligned}\int_{\mathcal{V}} \delta\mathbf{u}.\mathcal{B}(\mathbf{u}, \delta\mathbf{u})dV &\leq |\nabla\delta\mathbf{u}|_{L^2} |\mathbf{u}|_{L^\infty} \\ &\leq -\frac{\nu}{2}\int_{\mathcal{V}} \left(\nabla^2\delta\mathbf{u}\right).\delta\mathbf{u}\, dV + \frac{1}{2\nu}|\mathbf{u}|_{L^\infty}^2\end{aligned} \tag{2.11}$$

The first term is equal to half the viscous dissipation term with the opposite sign and the second term depends on the maximum velocity which we assumed to be bounded. When considering n disturbances, $\delta\mathbf{u}_i$ the trace of the linearized operator $\mathcal{A}$ on the subspace spanned by these disturbances can be expressed as:

$$Tr(\mathcal{A}P_n) = Tr(\mathcal{B}P_n) + Tr(\mathcal{L}P_n) \leq \frac{\nu}{2}Tr(\nabla^2 P_n) + \frac{\sigma B^2}{\rho}Tr(\nabla^{-2}\partial_{zz}^2 P_n) + \frac{n}{2\nu}|\mathbf{u}|_{L^\infty}^2 \tag{2.12}$$

This can be be written in dimensionless terms using L for distance, U_∞ the maximum velocity for velocity, $\sigma B U_\infty$ for electric current density and ν/L^3 for traces of operators:

$$Tr(\mathcal{A}P_n) \leq Tr\left(\frac{1}{2}\nabla^2 P_n + Ha^2\nabla^{-2}\partial_{zz}^2 P_n\right) + \frac{n}{2}Re^2 \tag{2.13}$$

where the Hartmann and Reynolds numbers are defined as $Ha = \sqrt{\sigma/(\rho\nu)}BL$ and $Re = U_\infty L/\nu$. This bound can be determined provided the trace of an operator nearly equal to the dissipative operator (viscous and Joule dissipation) can be evaluated. This is the subject of the next section.

3. Least dissipative modes in a flow between 2 Hartmann walls

In the expression for the trace of the linearized evolution operator (2.13), the last term is positive and depends only on the number of modes n and not on which modes are considered. The other term is the trace of a linear operator, consisting of half the viscous effect and of the entire Lorentz force. This term is negative and depends on the modes selected. In order to find an upper bound for the attractor dimension, we want to select the least dissipative terms so as to get as many as possible of them for before the trace vanishes. Finding least dissipative modes boils down to an eigenvalue problem.

3.1. *Eigenvalue problem*

In this section, we solve the eigenvalue problem for the dissipation operator $\mathcal{D}_{Ha}$ in a closed box with L-periodic boundary conditions in the x and y direction and impermeable walls of electric conductivity σ_W located at $z = -L$ and $z = L$. For these boundary conditions, the Laplacian operator is invertible so that the eigenvalue problem for the $\mathcal{D}_{Ha}$ operator can be formulated using non-dimensional variables as:

$$(\nabla^4 - 2Ha^2\partial_{zz}^2)\mathbf{v} = 2\lambda\nabla^2\mathbf{v} \tag{3.1}$$

$$\nabla.\mathbf{v} = 0 \tag{3.2}$$

Here lengths are normalised by L, velocities by an unspecified typical velocity U, the eigenvalues λ by ν/L^2 and electric currents by σBU. The choice of U is not important since the problem is linear. $\mathbf{v}$ also has to satisfy the same kinematic boundary conditions (2.7) as $\delta\mathbf{u}$. As in (2.8), an electric current field $\mathbf{J}$ is associated to $\mathbf{v}$ by:

$$\mathbf{J} = -\nabla^{-2}\partial_z\Omega \tag{3.3}$$

where $\Omega = \nabla \times \mathbf{v}$. $\mathbf{J}$ must be solenoidal and satisfy the same thin wall electric boundary conditions (2.9) as $\delta\mathbf{j}$ at the walls located at $z = -1$ and $z = 1$.
Since $\frac{\partial}{\partial x}$, $\frac{\partial}{\partial y}$ and $\frac{\partial}{\partial z}$ commute with $\mathcal{D}_{Ha}$, each component v_x, v_y and v_z of the solution $\mathbf{v} = (v_i)_{i\in\{x,y,z\}}$ of (3.1) is of the form:

$$v_i(\mathbf{x}) = V_i \exp(i\mathbf{k}_\perp.\mathbf{x}_\perp + \phi_i)Z_i(z) \tag{3.4}$$

with $\phi_i \in]-\pi, \pi]$ and $k_\perp^2 = k_x^2 + k_y^2$. The periodic boundary conditions in the x and y directions impose $(k_x, k_y) \in 2\pi\mathbb{Z}^2$. $Z_i(z) = \sum_j A_i^{(j)} \exp(K^{(j)}z)$ where $K^{(j)}$ are the complex roots of the dispersion equation obtained by inserting (3.4) into (3.1):

$$2\lambda = -(k_x^2 + k_y^2 + K^2) - 2Ha^2\frac{K^2}{k_x^2 + k_y^2 + K^2} \tag{3.5}$$

There are always two real and two imaginary roots for K: $1/\delta$, $-1/\delta$, $i\kappa_z$ and $-i\kappa_z$ with:

$$-\kappa_z^2 = Ha^2 + \lambda + k_\perp^2 - \sqrt{(Ha^2 + \lambda)^2 + 2k_\perp^2 Ha^2} \tag{3.6}$$

$$\frac{1}{\delta^2} = Ha^2 + \lambda + k_\perp^2 + \sqrt{(Ha^2 + \lambda)^2 + 2k_\perp^2 Ha^2} \tag{3.7}$$

Eventually, each function $Z_i(z)$ is of the general form:

$$Z_i(z) = A_i^1 \exp(z/\delta) + A_i^2 \exp(-z/\delta) + A_i^3 \exp(i\kappa_z z) + A_i^4 \exp(-i\kappa_z z) \tag{3.8}$$

Since the operator $\mathcal{D}_{Ha}$ self adjoint, there is a discrete spectrum of possible values of δ and κ_z, which is determined by the boundary conditions.

We shall now express the boundary conditions for the Z_i functions derived in the

previous section. The impermeability conditions at $z=-1$ and $z=1$ yield readily:

$$Z_i(-1)=0 \tag{3.9}$$
$$Z_i(1)=0 \tag{3.10}$$

which, by virtue of the continuity equation (3.1) implies:

$$Z'_z(-1)=0 \tag{3.11}$$
$$Z'_z(1)=0 \tag{3.12}$$

Using (**??**) to calculate $J_z(z=-1)$ and $J_z(z=1)$, then using the dispertion equation (3.5), the electric conditions at the walls located at $z=-1$ and $z=1$ are respectively written:

$$-k_x\left(Z'_y(-1)-(k_\perp^2+\lambda)\int Z_y(-1)\right)+k_y\left(Z'_x(-1)-(k_\perp^2+\lambda)\int Z_x(-1)\right)=0 \tag{3.13}$$

$$-k_x\left(Z'_y(1)-(k_\perp^2+\lambda)\int Z_y(1)\right)+k_y\left(Z'_x(1)-(k_\perp^2-\lambda)\int Z_x(1)\right)=0 \tag{3.14}$$

where $\int Z_i(z)=\delta a_i\exp(z/\delta)-\delta b_i\exp(-z/\delta)-ic_i/\kappa_z\exp(i\kappa_z z)+id_i/\kappa_z\exp(-i\kappa_z z)$.

3.2. *Squire and Orr-Sommerfeld modes*

We shall now use the boundary conditions (3.9), (3.10), (3.11),(3.12),(3.13) and (3.14) to find the sequences of values of δ, κ_z, λ as well as the properties of the related eigenmodes. Equations (3.9),(3.10),(3.11) and (3.12) impose 4 homogeneous conditions on the 4 coefficients A_z^1, A_z^2, A_z^3 and A_z^4 in the expression of Z_z. This means that the eigenmodes of the dissipation operator can be divided into two categories.

1) For the modes of the first category, conditions (3.9),(3.10),(3.11) and (3.12) are redundant so that $Z_z\neq 0$. In this case, the determinant formed by those 4 conditions must be zero, which yields:

$$\begin{aligned}&4\frac{\kappa_z}{\delta}+\cosh(\kappa_z+1/\delta)(\kappa_z-1/\delta)^2\\&-\cosh(\kappa_z-1/\delta)(\kappa_z+1/\delta)^2=0\end{aligned} \tag{3.15}$$

The sequence of values of κ_z and δ is determined by writing that $-\kappa_z^2$ and δ^2 must both be roots of the dissipation equation (3.5) for given values of Ha, λ, k_x and k_y. Eliminating λ between (3.7) and (3.6) yields the searched condition:

$$\frac{\kappa_z^2}{\delta^2}-k_\perp^2(k_\perp^2-\frac{1}{\delta^2}+\kappa_z^2+2Ha^2)=0 \tag{3.16}$$

The system formed by (3.15) and (3.16) admits exactly one solution for (κ_z,δ) in each interval $[p\pi/2,(p+1)\pi/2]\times]0,\infty[$ with $p\in\mathbb{Z}-\{0\}$. This defines the sequence of possible values of κ_z and δ for given Ha, λ, and $k_\perp$. This system admits exactly one solution for (κ_z,δ) in each interval $[p\pi/2,(p+1)\pi/2]\times]0,\infty[$ with $p\in\mathbb{N}-\{0\}$. The related eigenmodes have a non zero component along $\mathbf{e}_z$. By analogy with the eigenvalue problems which arise in the linear stability theory (see for instance), we shall call them *Orr-Sommerfeld* modes.

2) For the modes from the second category, conditions (3.13), (3.14),(3.11) and (3.12) are not redundant so that $Z_z=0$. The continuity then imposes that $k_xZ_x=-k_yZ_y$ so that the eigenmodes of this category are only determined by the 4 coefficients A_x^1, A_x^2, A_x^3,

and A_x^4 (or alternately A_y^1, A_y^2, A_y^3, A_y^4). δ and κ_z are then determined using the electric conditions at the walls (3.9) and (3.10) which together with (3.13) and (3.14) impose 4 homogeneous conditions on the 4 coefficients A_x^1, A_x^2, A_x^3 and A_x^4 : the determinant formed by these conditions has to be zero for the eigenmodes not to be trivial:

$$\begin{aligned}\left((\kappa_z^2-1/\delta^2)(\lambda_\perp^2-\kappa_z^2/\delta^2)+4\kappa_z^2/\delta^2\right)\sin(\kappa_z)\sinh(1/\delta)\\ +4Ha^2\kappa_z/\delta(\cos(\kappa_z)\cosh(1/\delta)-1)=0\end{aligned}\tag{3.17}$$

Here the system formed by (3.17) and (3.16) admits exactly one solution for (κ_z,δ) in each interval $[p\pi/2,(p+1)\pi/2]\times]0,\infty[$ with $p\in\mathbb{Z}$. The related eigenmodes have no velocity component along $\mathbf{e}_z$ and those with $\kappa_z<\pi/2$ exhibit only a weak dependence on z so that we may identify them as quasi two-dimensional modes. Following our analogy with linear stability problems, we shall name the modes of this second category *Squire* modes.

These modes can be explicited by finding the three independent coefficients from A_x^1, A_x^2, A_x^3, and A_x^4. This is done by solving the system formed by (3.9), (3.10),(3.11) and (3.12), which is at most of rank 3. Z_y is obtained by $k_yZ_y=-k_xZ_x$ and $Z_z=0$. The associated eigenspace has therefore a dimension between 1 and 3.

In summary, for a given value of Ha, the eigenvalues $\lambda(k_\perp,\kappa_z)$ of the operator $\mathcal{D}_{Ha}$ are given by the dissipation equation (3.16), where $k_\perp=\sqrt{k_x^2+k_y^2}$ with $k_x,k_y\in\mathbb{Z}$. For a fixed value of $k_\perp$, κ_z takes one value in $]0,\pi/2[$ and 2 values in each interval $]p\pi/2,(p+1)\pi/2[$ with $p\in\mathbb{Z}-\{0\}$. This defines a discrete sequence of values for λ, which once sorted by increasing module yields the sequence of the least dissipative eigenmodes of the dissipation operator $\mathcal{D}_{Ha}$. At this point, the eigenmodes of the dissipation operator already exhibit a quite remarkable similarity with the known properties of a flow between 2 parallel plates as each of those modes exhibits "core" velocity fluctuations of wavelength κ_z as well as an exponential boundary layer

3.3. *Numerical results*

By sorting the values of $\lambda(k_\perp,\kappa_z)$, we are now able to find the minimum of $|\langle\mathcal{D}_{Ha}P_n\rangle|$ for any given value of n. We shall now perform this task numerically since the values of κ_z cannot be found analytically. An upper bound for the attractor dimension as a function of Ha and Re then follows immediately. The numerical method is the same as the one already used in the case of a box with 2π-periodic boundary conditions in the 3 directions of space : it consists of sweeping the $(k_\perp,\kappa_z)$ plane with the iso-dissipation (iso-λ) curves, starting at $|\lambda|=0$. For each value of λ, we count the number of $(k_\perp,\kappa_z)$ points enclosed in the corresponding iso-λ curve and calculate the sum of λ over all of those points. Each point corresponds to an eigenvalue and should therefore be weighed by its multiplicity both when counting those points and building this sum. However it is simpler to build the sum by taking all multiplicities equal to one. The obtained sum for a given value of n is a slightly looser lower bound for $|\langle\mathcal{D}_{Ha}P_n\rangle|$, but this may only affect the numerical constants appearing in the final results, and not the dependence on Ha, n and Re.

The difference between the present case with walls at $z=-1$ and $z=1$ and the periodic case is that the sequence of real values of κ_z replaces that of k_z in the periodic case, which has integer values. It is important to notice that the only imprecision brought by the numerical process is that of the truncation on the sequence of numerical values of κ_z and λ, as well as that which results from the resolution of the systems of equations $\{(3.15),(3.16)\}$ and $\{(3.17),(3.16)\}$ using the Newton method. However, since each so-

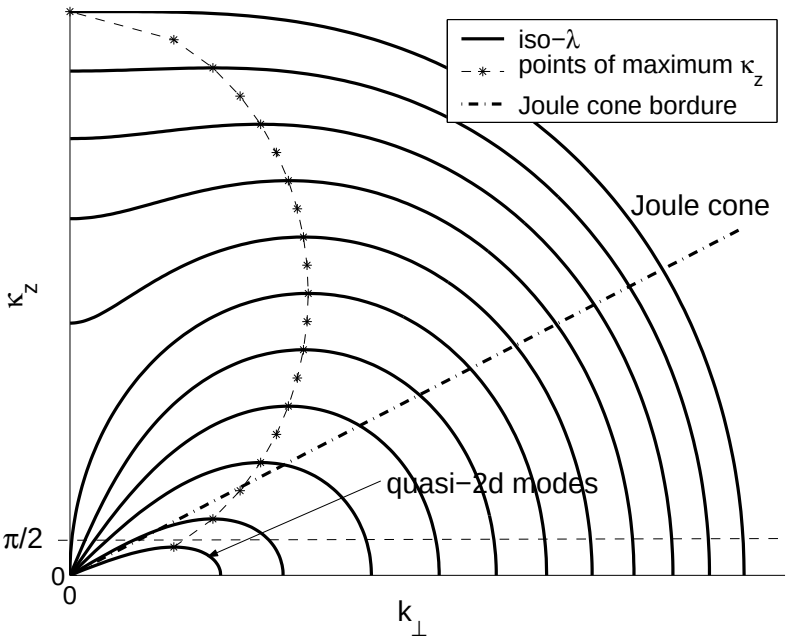

FIGURE 1. Iso-dissipation curves in the Fourier space (one point represents all the eigenmodes with the same $(k_\perp, \kappa_z)$). each curve encloses the set of the n least dissipative modes of a given n. The properties (anisotropy and size of the smallest scales) from the class of flows decomposed on this set of modes can be read from the shape of the iso-λ_m curve corresponding to the value of n relating to the considered flow.

lution of the system is bracketed, there is no risk of finding any spurious eigenvalues. In this sense, the method can be considered to give an exact result. It should also be pointed out that contrarily to the periodic case where k_z has integer values, finding the sequence of values of κ_z requires high precision arithmetics since the numbers involved in (3.15) and (3.17) are very high, although the values of κ_z are not. Using the LONG DOUBLE type in C language allows us to reach values of Ha up to 5000 and 10^5 modes. Computing the sequence of minimal modes for higher values of Ha and n would require to use multi-precision libraries.

The numerical algorithm yields directly the minimum of $|\langle \mathcal{D}_{Ha} P_n \rangle|$, $k_{\perp_m}$, κ_{z_m}, δ_{min}, δ_{max}, as well as the transition between quasi-2d and 3d sets of modes as a function of n and Ha. The value of n for which the trace of the total evolution operator is zero (*i.e.* $\langle((-\mathcal{D}_{Ha} + \mathcal{B}(., \mathbf{u}))P_n)\rangle = 0$) is an upper bound for the attractor dimension. Knowing the minimum of $|\langle \mathcal{D}_{Ha} P_n \rangle|$ and using (**??**), the value of Re for which n is an upper bound for d_M is given by $Re = \sqrt{|\langle(\mathcal{D}_{Ha} P_n)\rangle|/n}$. The results are plotted on figures 2, **??** and **??**.

4. Dimension and modes of 3D MHD attractors

4.1. *Set of the least dissipative modes and attractor dimension*

Because the function $\lambda(k_\perp, \kappa_z)$ has the same expression as the function $\lambda(k_\perp, k_z)$ in the case with periodic boundary conditions in the 3 directions of space, the upper bound for the attractor dimension $d_M(Ha, Re)$ in both cases have similar behaviour. As in the periodic case, the maximum values $k_{\perp_m}$ and κ_{z_m} over the set of the n least dissipative

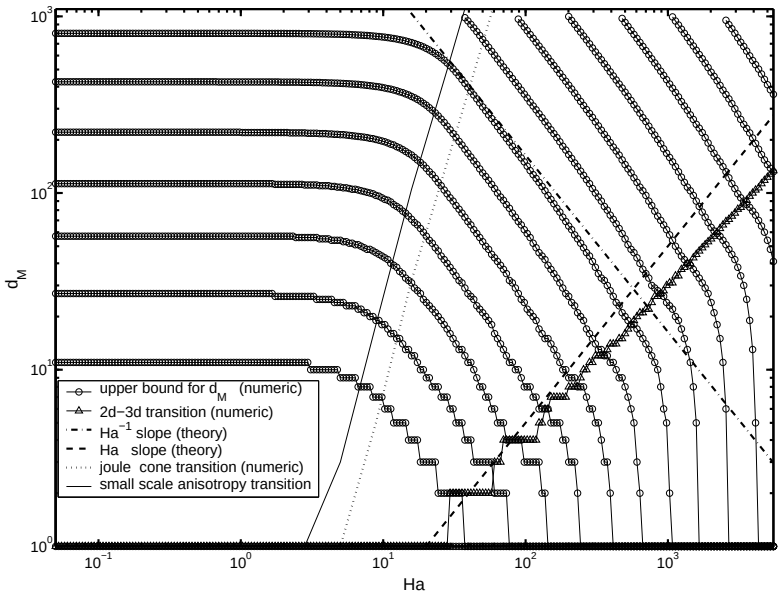

FIGURE 2. Attractor dimension as a function of Ha for fixed values of Re. 3 regions appears which correspond to 3 types of flows: 3d quasi-isotropic, 3d anisotropic, and quasi-2d. Note that the attractor dimension is strongly over-estimated in the quasi-2d case as the upper bound **??** applies to all flows (3d). It can be improved in the case of quasi-2d flows as shown in section 5

modes of $k_\perp$ and κ_z can be deducted from the geometrical shape from the $\lambda(k_\perp, k_z) = \lambda_m$ curve, where λ_m is associated to the most dissipative mode of the set (see figures 1 and **??**). If the velocity field is expanded over the least dissipative modes, $k_{\perp_m}$ and κ_{z_m} represent the sizes of the dissipative scales in the direction perpendicular and parallel to the magnetic field respectively. It is therefore interesting to compare them to their heuristic counterpart obtained from Kolmogorov-like arguments as here, $k_{\perp_m}$ and κ_{z_m} are obtained without any additional assumption on the Navier-Stokes equations. This is done in the next section.

Increasing progressively the values of Ha for a given value of Re, the upper bound for the attractor dimension exhibits three different behaviours which correspond to a 3d isotropic flow, a 3d anisotropic flow and quasi-2d flow respectively. For low values of Ha, d_M varies little with Ha and the set of eigenmodes of the dissipation which achieve the upper bound is located in a circle centred on the origin in the $(k_\perp, \kappa_z)$ plane. If one imagines a flow represented by such modes, it would be 3d and nearly isotropic. For higher values of Ha, $d_M \sim Ha^{-1}$, just like in the case with periodic boundary conditions. The least dissipative modes are located within a cardioid-shaped curve, with no modes in the vicinity of the κ_z axis. The related flow is strongly anisotropic with vortices elongated in the z direction. The transition between those first two types of flows can be characterised by the disappearance (*resp.* appearance) of the last (*resp.* first) mode of the form $(k_\perp = 0, \kappa_z \neq 0)$. When such modes exist, the tangent at the origin of the iso-λ curve corresponding to the most dissipative set of eigenmodes which achieve the upper bound for d_M can be defined. All modes are then located under this line which matches the concept of "Joule Cone" described by : in the existing theories of turbulence, the energy-containing modes are expelled from this cone of axis $(0, k_z)$ in the Fourier space for high values of Ha.

The present case with walls at $z = -1$ and $z = 1$ differs from the periodic case for

higher values of Ha, for which the related set of minimal eigenmodes of the dissipation is quasi-two dimensional. In the periodic case, those modes all satisfy $k_z = 0$ so that they are strictly two-dimensional and produce no Joule dissipation. In this case, d_M doesn't vary anymore when Ha is increased. In the case with walls, the quasi two dimensional modes are Squire modes with $0 < \kappa_z < \pi/2$ which exhibit an exponential velocity profile in the vicinity of the wall. This means that the associated values of $|\lambda|$ are higher in the case with walls. When the least dissipative modes are all quasi-2d Squire modes, some dissipation still arises because of the presence of the boundary layer profile at $z = 1$ and $z = -1$. This results in d_M decreasing rapidly as Ha increases, contrarily to the periodic case. The boundary layer properties of the least dissipative modes are more specifically studied in section 4.3. Also, since the upper bound for the trace of the operator associated to the inertial terms (**??**) is a general one which relies on no particular assumption on the flow's possible three-dimensionality, it becomes unrealistic when the flow becomes two-dimensional. An improved upper bound for the attractor dimension in the quasi-2d case is therefore derived in section 5, using a quasi two-dimensional model.

4.2. *Analytic approximation for the upper bound for d_M*

We shall now derive some analytical estimates for the attractor dimension so as to be able to further compare our results to the results for the size of the dissipative scales available from .

As the modes are spread uniformly in the Fourier space, with $1/\pi^3$ modes per unit of volume, the value of λ_m can be found by writing that in the $1/8^{th}$ space $k_x > 0, k_y > 0, \kappa_z > 0$, the volume enclosed by the iso-λ_m curve should be $n/(8\pi^3)$. For sufficiently high values of κ_{z_m} and $k_{\perp_m}$, this can be expressed using integrals:

$$8\pi^3 \int_{V_{\lambda_m}} dk_x dk_y dk_z = n \tag{4.1}$$

The trace of $\mathcal{D}_{Ha} P_n$ similarly expresses as:

$$(\mathcal{D}_{Ha} P_n) = 8 \int_{V_{\lambda_m}} \lambda(k_x, k_y, k_z) dk_x dk_y dk_z \tag{4.2}$$

The set of n least dissipative modes in the Fourier space is enclosed in the same iso-λ curve as the set of $8n/\pi^3$ least dissipative modes in the $2\pi-$periodic case. The attractor dimension and the corresponding values of $k_\perp^{max}$ are then found by replacing n with $8n/\pi^3$ in the results from study with periodic walls (, p3176). Two distinct cases are found:

If the set of least dissipative modes is located within an elongated cardioid with no mode of the form $k_\perp = 0$, then the Joule cone of axis $(O\kappa_z)$ exits and its half-angle it that of the tangent at the origin of the iso-λ_m curve:

$$\sin\theta_m = \sqrt{\lambda_m / Ha^2} = 2^{1/4} 2\pi^{-5/4} n^{1/4} Ha^{-3/4} \tag{4.3}$$

All modes are located outside of this cone in the Fourier space. In this case, the upper bound for the attractor dimension is:

$$d_M \leq \frac{9\pi^5}{256} \frac{Re^4}{Ha} \tag{4.4}$$

and the related bounds for $k_{\perp_m}$ and κ_{z_m} are:

$$k_{\perp_m} \leq \left(\frac{3}{2\pi^2}\right)^{1/4} Re \tag{4.5}$$

$$k_{z_m} \leq \left(\frac{3}{2\pi^2}\right)^{1/2} \frac{Re^2}{Ha} \tag{4.6}$$

These sets of modes describe a 3d anisotropic flow, for which heuristic considerations of the Kolmogorov type predicts $d_M \sim Re^2/Ha$, $k_{\perp_m} \sim Re^{1/2}$ and $k_{z_m} \sim Re/Ha$ (see).
In the case where no Joule cone can be defined within the set of dissipative mode, the related flow is quasi-isotropic with:

$$d_M \leq \frac{5\pi^4\sqrt{30}}{216} Re^3 \left(1 - \frac{2}{3}\frac{Ha^2}{Re^2}\right)^{3/2} \tag{4.7}$$

and corresponding k_{z_m} and κ_{z_m}:

$$k_{\perp_m} = \pi\sqrt{5} Re \left(1 - \left(\frac{2}{9} + \frac{1}{15\pi^2}\right)\frac{Ha^2}{Re^2}\right)^{1/2} \tag{4.8}$$

$$\kappa_{z_m} = \pi\sqrt{5} Re \left(1 - \left(\frac{2}{9} + \frac{4}{15\pi^2}\right)\frac{Ha^2}{Re^2}\right)^{1/2} \tag{4.9}$$

In the limits of small Hartmann numbers, (4.7) recovers the classical hydrodynamic bound for 3d turbulence (**??**). The transition between the 3d quasi-isotropic and 3d anisotropic flow can be characterised by the appearance of the Joule cone which happens when $\sin\theta_m = 1$, *i.e.*:

$$\frac{Ha}{Re} = \frac{\sqrt{3}}{2^{-3/4}} \tag{4.10}$$

As in the periodic case, the bounds for d_M, $k_\perp$ and κ_{z_m} exhibit the same dependence on Ha as the heuristic predictions which suggests that our estimate renders the effect of the Lorentz force on the small scales realistically. The powers of Re are however overestimated, but this can be inferred to the estimate for the expansion rate of the inertial terms (**??**) which is known to be too high. As mentioned in section **??**, the problem of finding an optimal estimate for these terms is to this day still open.
In the two cases of 3d flow with and without Joule cone, the upper bound for the attractor dimension exhibits the same dependence on the non-dimensional numbers as in the case with periodic boundary conditions. This confirms the tendency already observed on the numerical results from the previous section. It also suggests that problems with periodic boundary conditions in the 3 directions of space provide some scaling laws which are relevant to cases involving more realistic boundary conditions such as walls as long as the velocity field is strongly three dimensional. This relevance however breaks down for quasi two-dimensional velocity fields, the dynamics of which is controlled by the boundary layers which arise along the walls perpendicular to the magnetic field.

4.3. *Boundary layer properties*

We now turn our attention to the influence of the walls on the modes minimising the dissipation, as there lies the most important difference between the periodic case and the case with walls. More precisely, we shall study the values of the boundary layer thickness δ which characterises the eigenmodes of the dissipation.
As mentioned in section 3.1, each mode (k_x, k_y, κ_z) can alternately be represented by the

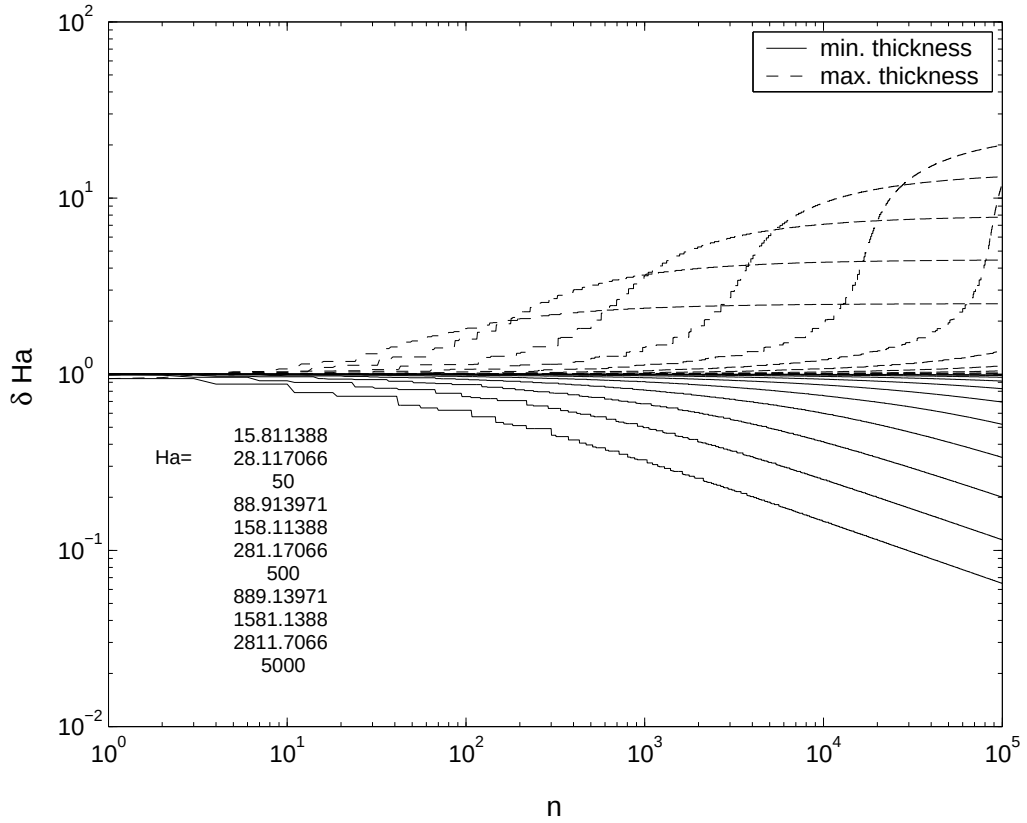

FIGURE 3. Maximum and minimum of the boundary layer thickness δ for n the set of modes which minimise the dissipation, as a function of n, for different values of Ha. For each Ha, a transition appears between a state where all modes have a boundary layer thickness close to $1/Ha$ and states for which a broader spectrum of values of δ is present. The value of n at which characterises the transition takes place increases with Ha.

triplet (k_x, k_y, δ). Figure 3 represents the evolution of the minimum (resp. maximum) value of δ reached within the set of the n least dissipative modes δ_{min} (resp. δ_{max}) as a function of n, obtained numerically from $\{(3.15), (3.16)\}$ and $\{(3.17), (3.16)\}$. For each fixed value of Ha, there appears a transition between two types of sets of least dissipative modes: for low values of n, all modes are characterised by a value of δ close to $1/Ha$ whereas for higher values of n, the set of least dissipative modes exhibits a much broader spectrum of values of δ. A velocity field represented by a combination of modes taken before this transition would exhibit a laminar boundary layer of thickness $1/Ha$, with an exponential profile. This matches exactly the prediction of the laminar Hartmann layer theory introduced in section **??**. After the transition, some modes appear with a thicker boundary layer, as well a modes with a layer much thinner than $1/Ha$. This two-layer structure strongly resembles that of the theoretical prediction of for the turbulent Hartmann layer, which also involves such a double deck structure, with a viscous sublayer.

In order to quantify how this transition depends on the parameters Ha, n and Re, we define the latter quantitatively as the intersection between the line $\delta Ha = 1$ (see 3) and the asymptote to the curve $\delta_{min}(n)$ for each value of Hartmann and we have plotted the result on figure 4. It is remarkable that the transition to turbulence withing the Hartmann layer never occurs in quasi-2d flows, but only when 3d modes are present. This

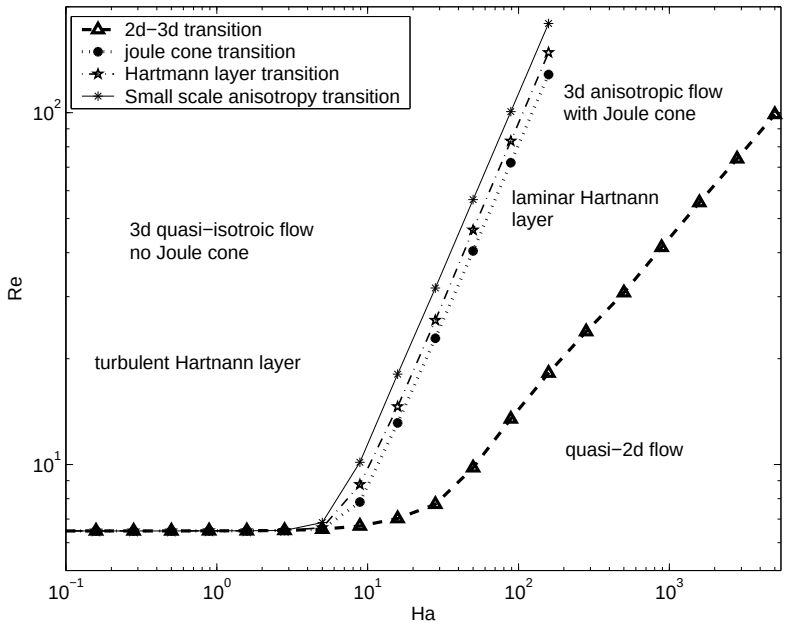

FIGURE 4. Map of the different types of turbulence (a) in (Ha, n) plane, (b) in (Ha, Re) plane

strong property is very different to the results of who studied numerically the transition to turbulence of the Hartmann layer in channel flows and found that there can exist a two-dimensional region outside of the turbulent Hartmann layer. If the behaviour of the least dissipative modes does indeed represent that of the real flow, this suggests that the destabilisation of the Hartmann layer may follow different scenarios whether there is an average outer velocity, as in channel flows, or not, as in the present study. There is to this day no experimental nor theoretical answer to this question.

These numerical results can be supported by some analytical expressions for the minimum and maximum boundary layer thickness, which can be obtained by eliminating $k_\perp^2$ between (3.6) and (3.7). This defines the iso-λ curves in the (δ, κ_z) plane, which enclose the set of least dissipative modes. Then remarking that the maximum and minimum values of δ are obtained for $\kappa_z = 0$ yields the expressions for δ_{min} and δ_{max} †:

$$\delta_{min} = \frac{1}{\sqrt{Ha^2 - \lambda_m}} \tag{4.11}$$

$$\delta_{max} = \frac{1}{\sqrt{Ha^2 + \lambda_m}} \tag{4.12}$$

In the case of a 3d set of modes with Joule cone ($Ha \leq \lambda_m \leq Ha^2$), δ_{min} and δ_{max} are expressed as functions of Ha and Re using (4.3) and (4.4):

$$\delta_{min} = \frac{1}{Ha\sqrt{1 + \frac{Re^2}{Ha^2}}} \tag{4.13}$$

$$\delta_{max} = \frac{1}{Ha\sqrt{1 - \frac{Re^2}{Ha^2}}} \tag{4.14}$$

† κ_z is never zero so these values of δ_{min} and δ_{max} are never reached: δ_{max} is a close upper bound and δ_{min} is a close lower bound.

For low Reynolds numbers (or low values of $|\lambda_m|$ in (4.11)) and (4.12), δ_{min} and δ_{max} are very close to each other, whereas they separate quickly when $\frac{Re}{Ha}$ approaches unity, as confirmed by the numerical results on figure 4. Remarkably, this boundary layer transition coincides approximately with the disappearance of the Joule cone (4.10).
As for the turbulent quantities discussed in section 4.1, the boundary layer properties of the least dissipative modes exhibit some striking similarities with that of existing theories . Quantitatively, the boundary layer thickness associated to those modes has the same dependence on Ha as that of real Hartmann layers even though the overestimation of the expansion rate of the inertial terms (**??**) impairs the dependence on Re of δ. This adds up to the conclusion of which found that the set of least dissipative modes in a 3d periodic box bears the same behaviour as the real turbulent low (Joule cone angle, small scales, transition between 2d and 3d turbulence). Indeed, when walls are present, not only are the turbulent properties also recovered, but also the fine properties of the Hartmann boundary layers are closely mimicked by the least dissipative modes.

5. Attractor dimension for a 2D MHD model

To conclude this search of an upper bound for the attractor dimension of a turbulent MHD flow in a box with Hartmann walls, we shall now derive a tighter bound in the case where the flow is two-dimensional by using quasi-2d motion equations. Such equations are often used to model quasi two-dimensional flows between two parallel insulating planes. They are obtained by averaging the full 3d Navier-Stokes equations along the direction of the magnetic field between the two planes. The model is closed by assuming a particular velocity profile along this direction. were the first to propose such a model, in which this particular velocity profile was derived from first order matched asymptotics using the small parameters $1/Ha$ and $1/N$. At this order, The velocity profile does not vary along the direction of the magnetic field, except in the vicinity of the walls where Hartmann boundary layers of thickness $1/Ha$ develop with an exponential velocity profile. For a distance $2L$ between the Hartmann walls, the resulting model can be written as follows:

$$\frac{\partial}{\partial t}\mathbf{u} + \mathbf{u}\cdot\nabla\mathbf{u} + \frac{1}{\rho}\nabla p = \nu\nabla^2\mathbf{u} - \frac{1}{t_H}\mathbf{u} + \mathbf{f} \tag{5.1}$$

where the Hartman friction time is defined as $t_H = (L^2/\nu)(1/Ha)$ and where the two-dimensional velocity field $\mathbf{u}$ is solenoidal.
Even though this model is obtained at the cost of an approximation on the full 3d equations, the properties of the related dynamical system are still interesting to investigate since this model has proven its accuracy in many instances ; ; . We shall now derive an upper bound for the attractor dimension d_{SM} for the related problem with $L-$periodic boundary conditions in the two directions of space $\mathbf{e}_x$ and $\mathbf{e}_y$.
The only difference between (5.1) and the two-dimensional Navier-Stokes equation is the dissipation term, with related operator $\mathcal{D}_{SM} = \nu\nabla^2 - 1/t_H\mathcal{I}$, where $\mathcal{I}$ is the identity. Application of the method described in section **??** yields an upper bound for the growth rate of any $n-$dimensional volume located in the vicinity of the attractor:

$$\langle \mathcal{A}P_n\rangle = \langle \mathcal{B}(\cdot,\mathbf{u})P_n + \mathcal{D}_{SM}P_n\rangle \tag{5.2}$$

Using $\mathcal{D}_{SM}P_n = -\nu m - n/t_H$ and the estimate (**??**) for the 2d inertial terms, this simplifies in:

$$\langle \mathcal{A}P_n\rangle \leq \nu\left(\frac{m}{2} - cC^{4/3}(1+logC)^{2/3}\right) + \frac{n}{t_H} \tag{5.3}$$

where $C = L^2/(4\pi^2\nu)\sup_{\mathbf{u}}\langle|\nabla^2\mathbf{u}|^2\rangle^{1/2}$. As $m \geq (4\pi^2/L)n^2$, the largest root of $\nu\left(\frac{4\pi^2}{L^2}n^2 - cC^{4/3}(1+logC)^{2/3}\right)+\frac{n}{t_H}$ provides an upper bound for the attractor dimension:

$$d_{SM} \geq -\frac{Ha}{2\pi} + \sqrt{\frac{Ha^2}{4\pi^2} + 4cC^{4/3}(1+logC)^{2/3}} \tag{5.4}$$

The lower bound for the trace of the operator $1/t_H\mathcal{I}$ is in fact its exact value. Since the estimate for the trace of the inertial term derived for the classical 2d theory is known to be log-optimal, the final bound (5.4), can be reasonably expected to be just as optimal.

Two limit cases are of interest: for $Ha = 0$, the two-dimensional Navier-Stokes equation is recovered and so is the upper bound for the dimension of the related attractor as the $l.h.s.$ of (5.4) tends to $2cC^{2/3}(1+logC)^{1/3}$. This has however no significance in the framework of 3d MHD flows confined between two walls as a flow without magnetic field would in fact be three-dimensional. The case $Ha/C^{2/3} >> 1$ is more interesting as it applies when the magnetic field is strong, which is a necessary condition to obtain a quasi-2d flow as confirmed in section 4.1 (see for instance figure 2). In this case, the upper bound writes approximately as $\frac{2cC^{4/3}(1+logC)^{2/3}}{Ha}$.

Finally, as (5.4) provides a relation between n, the number of modes present in the flow, C and Ha for a quasi two-dimensional flow, the 2d-3d transition obtained numerically in section 4.1 as a function of n and Ha can also be expressed in terms of C and Ha. The result is reported on figure 5 . Since (5.4) can reasonably be expected to be log −optimal, so can be the quasi-2d-3d transition. The curve suggest that for sufficiently big Hartmann numbers, the transition occurs approximately for $C \sim Ha^{3/2}$. This prediction for the transition between quasi-2d and 3d MHD turbulence has the advantage to be comparable to experiments as the case with walls studied here corresponds to realistic experimental conditions. To be able to perform such a comparison, we need to relate C to the parameters Ha and $\mathcal{G}$. The inequality $C \leq \mathcal{G}$ shown by still holds in the present case but some order of magnitude analysis on the energy budget associated to (5.1) rather suggests that $C \sim \mathcal{G}/(1+Ha)$, which would imply that the attractor dimension of a quasi two-dimensional MHD flow varies as $\mathcal{G}^{4/3}Ha^{-7/3}[1+log(\mathcal{G}/Ha)]^{2/3}$ for large values of Ha. In this case, the quasi-2d-3d transition should occur for $\mathcal{G} \sim Ha^{5/2}$ and the the smallest lengthscale in the flow would vary as $k_{\perp_m} \sim G^{2/3}/Ha^{1/2}$.

6. Concluding remarks

REFERENCES

Kolmogorov A, N. Local structure of turbulence in an incompressible fluid at very high Reynolds numbers. *Dokl. Akad. Nauk. SSSR*, 30:299–303, 1941.

T. Alboussière and R. J. Lingwood. A model for the turbulent Hartmann layer. *Phys. Fluids*, 12(6):1535–1543, 2000.

L. Bühler. Instabilities in quasi two-dimensional magnetohydrodynamic flows. *J. Fluid Mech.*, 326:125–150, 1996.

P. Constantin, C. Foias, O.P. Mannley, and R. Temam. attractors representing turbulent flows. *Mem. Am. Math. Soc.*, 53,314, 1985.

P. Constantin, C. Foias, O.P. Mannley, and R. Temam. determining modes and fractal dimension of turbulent flows. *J. Fluid. Mech.*, 150:427–440, 1985.

P. Constantin, C. Foias, and R. Temam. on the dimension of the attractors in 2d turbulence. *physica D*, 30:284–296, 1988.

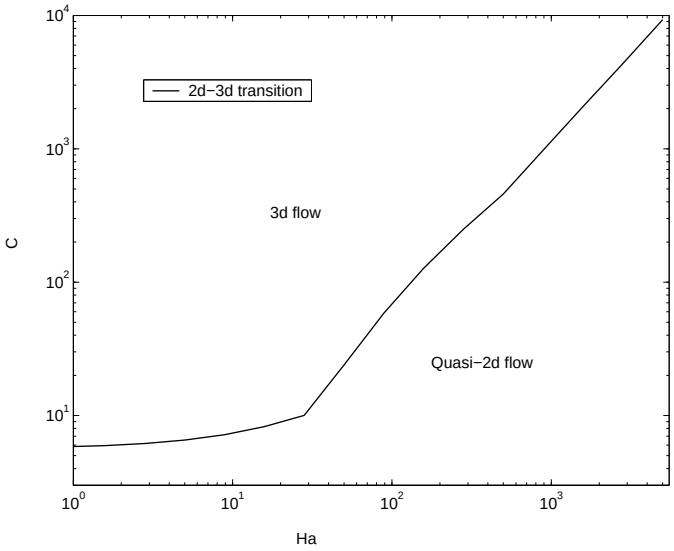

FIGURE 5. Transition 2d-3d in the C-Ha plane.

C.R Doering and J. D. Gibbons. *Applied analysis of the Navier-Stokes equation*. Cambridge University Press, 1995.

P. G. Drazin and W.H. Reid. *Hydrodynamic stability*. Cambridge university press, 1995.

R.H. Kraichman. Inertial ranges in two-dimensional turbulence. *Phys. Fluids*, 10, 1967.

D. Krasnov, E. Zienicke, O. Zikanov, T. Boeck, and A. Thess. Numerical study of the instability of the Hartmann layer. *J. Fluid Mech.*, 504:183–211, 2004.

R. Moreau. *Magnetohydrodynamics*. Kluwer Academic Publisher, 1990.

A. Pothérat and T. Alboussière. Small scales and anisotropy in low-Rm MHD turbulence. *Phys. Fluids*, 15 (10):1370–1380, 2003.

A. Pothérat, J. Sommeria, and R. Moreau. An effective two-dimensional model for MHD flows with transverse magnetic field. *J. Fluid Mech.*, 424:75–100, 2000.

A. Pothérat, J. Sommeria, and R. Moreau. Numerical simulations of an effective two-dimensional model for flows with a transverse magnetic field. *J. Fluid. Mech*, 534:115–143, 2005.

Joël Sommeria and René Moreau. Why, how and when MHD turbulence becomes two-dimensional. *J. Fluid Mech.*, 118:507–518, 1982.